7D.7 TROPICAL CYCLONES RISK MODELS – CIRCULAR SYMMETRY REVISITED

Peter J. Sousounis*, Jason Butke, and Kevin Hill
AIR Worldwide Corporation, Boston, MA

1. INTRODUCTION

From a catastrophe modeling standpoint, accurate simulation of tropical cyclone (TC) winds in terms of the maximum wind speed, the distance at which they occur, and how they decay outward (and inward) from the radius of maximum winds are important features for correctly modeling the damage from TCs. Whether those maximum winds occur on the left, right, front, or back of the storm is also an important consideration, given that property along the coast and inland is non-uniformly distributed and valued.

Because of the typically hundreds of thousands of events they must simulate, many catastrophe models are inherently parametric in nature and therefore must make simplifying assumptions. For example, they typically assume that TCs have a circularly symmetric rotational wind field and that the forward speed imposes the only horizontal asymmetry, which leads to the strongest winds being on the right-hand side for northern hemisphere storms.

However, observational and modeling studies show that wind asymmetries can stem from embedded mesoscale circulations like tornadoes (Schultz and Cecil 2009), environmental wind shear (Frank and Ritchie 1999), adjacent weather systems (Persing et al. 2002), and extratropical transitioning (XTT, Klein et al. 2002, Chen and Yau 2003). The latter is a typical feature of storms affecting Japan. Over 60% and nine of the top ten loss causing events that have affected Japan undergo XTT within 500 km of the coastline (Sousounis and Butke 2010). The transitioning process typically leads to the formation of fronts that can significantly skew the symmetry. In some cases, the evolution leads to the formation of strongest winds on the left hand side, which can conflict with the assumption that strongest winds from a TC are on the right hand side and which can lead to inaccuracies in the modeled damage for a particular storm and also for the overall risk of a particular region.

Typhoon Tokage 2004 provides a good example of an asymmetric typhoon that affected Japan. According to the Japanese Meteorological Agency (JMA), Tokage made landfall on Shikoku Island at 06 UTC 20 October 2004 with a central sea-level pressure (SLP) of 950 hPa and 75 kt winds (10 min sustained) as shown in Fig. 1. Available observations from the Automated Meteorological Data Acquisition System (AMeDAS) show strongest winds near the center at that time were on the right-hand side (RHS). But, because Tokage was undergoing XTT, its interaction with an upper level jet streak enhanced ageostrophic winds at the surface so that strong winds developed on the left hand side (LHS) – as its central pressure was rising (Sousounis and Desflots 2010). Tokage caused approximately one billion USD in insured loss according to the General Insurance Agency of Japan (GIAJ). A significant portion of it (i.e., 25-40%) was from precipitation induced flooding and strong winds on the left (west) coast of Japan.

It is likely that there are other storms similar to Tokage – in the sense that strong winds develop on the left hand side. But, since not all storms that undergo XTT develop strong winds on the LHS, and since not all storms that develop strong winds on the LHS undergo XTT, it is important to understand some key aspects regarding the climatology of asymmetric TCs so that these features can be incorporated into TC catastrophe models.

As a step in that direction, this study examines the climatological frequency with which typhoons affecting Japan exhibit maximum winds on the LHS. It also examines the synoptic scale environment under which a left-hand maximum wind (referred to as Left Max throughout the remainder of this paper) occurs. Both of these features are important to understand so that wind field asymmetries can be incorporated more accurately into the parametric wind field calculation of TC catastrophe models.

2. IMPORTANCE OF ASYMMETRY FOR CATASTROPHE MODELING

One may justifiably argue that stochastically modeling the wind damage from storms with random asymmetries is not so significant – *if* the asymmetries are truly random or very weak. However, the key phrase *truly random or very weak* is important to consider. If an equal number of storms that affect an area have strongest winds on the left as on the right, then in the aggregate sense, this argument may be

* *Corresponding author address:* Peter J. Sousounis, AIR-Worldwide Corporation., 131 Dartmouth Street, Boston, MA 02116; email: psousounis@air-worldwide.com.

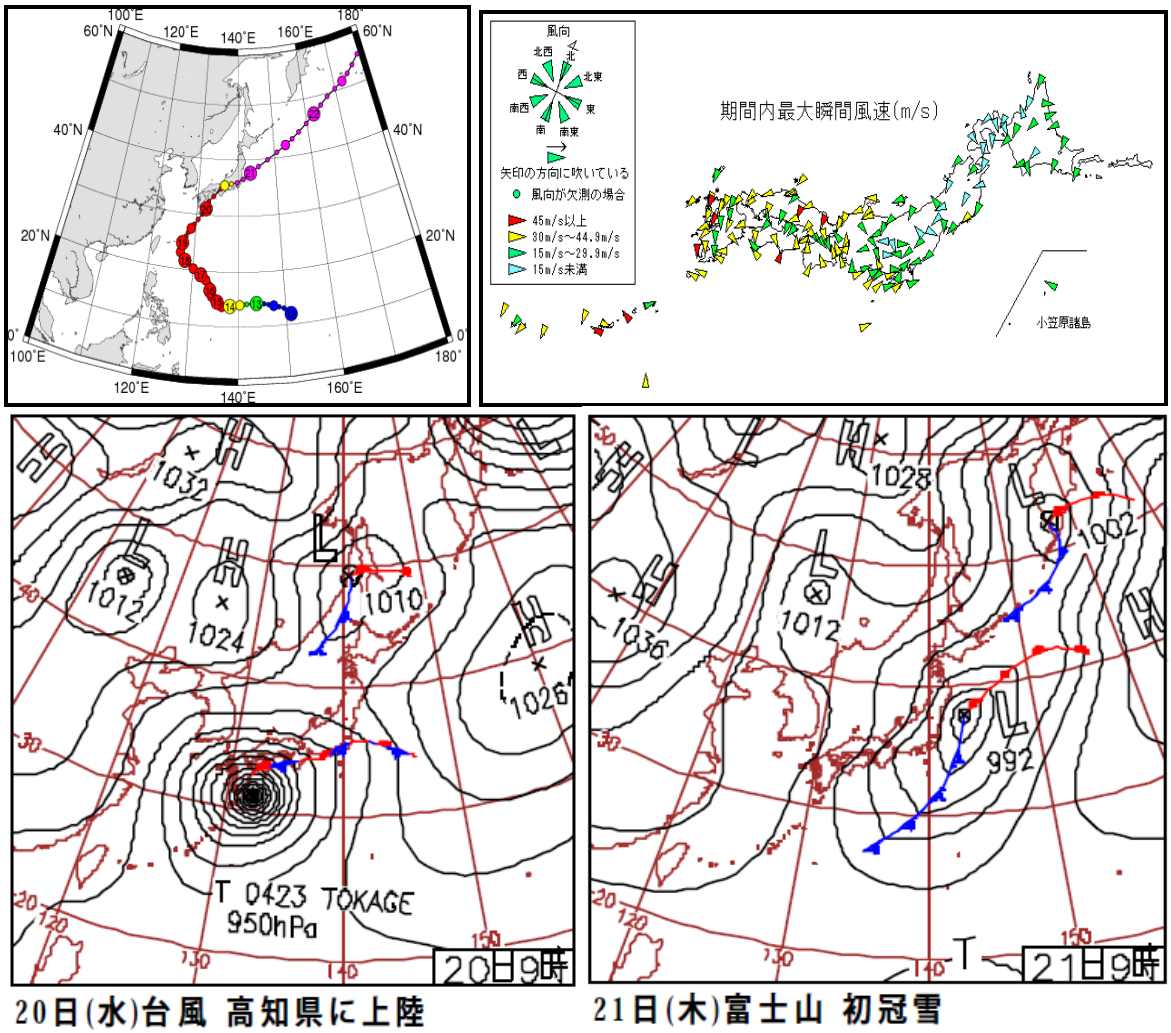

Fig. 1. Characteristics of Tokage 2004. Storm track as indicated by the JMA (upper left). Maximum observed wind speeds (3s gust in m/s) and direction (upper right). Sea level pressure and frontal locations 6 hours prior to landfall at 09 JST 20 Oct 2004 (lower left) and 18 hours after landfall 09 JST 21 Oct 2004 (lower right). Images adapted from Digital Typhoon – http://agora.ex.nii.ac.jp/digital-typhoon/index.html.en.

valid[2]. Also, if the asymmetries are insignificant, then this argument may be valid. However, if the climatology of such asymmetries is other than random, or shows significant magnitude, then accounting for such is important in formulating an accurate picture of the TC risk for a particular region. Additionally, many catastrophe modeling agencies are called upon by their clients during significant TC events to provide an estimate of expected insured losses. In such cases it is also important to account for any asymmetries and maximize the accuracy of the modeled wind speed so as to maximize the accuracy of the modeled expected loss.

Differences can be significant. As an example, we used our AIR Japan Typhoon Loss Model and two versions of the Tokage wind field. One version was based on a circularly symmetric rotating vortex with the forward speed added in a conventional manner – to create a version with maximum winds on the RHS (right-max). A second was based on the same vortex but with the same forward speed added in the opposite direction to create a version with maximum winds on the LHS (left-max). Because of the particular track, a broader region of strong winds extended north and west of Tokage in the left-max version. The stronger winds to the left, coupled with the fact that Tokyo was exposed to Tokage's right side, led to the wind losses being much higher for the left max version – by about a factor of two.

Because a goal of this study is to learn more about how often and where such TC-scale asymmetries in the wind field occur, and because

[2] Even in this case, given the nonlinear dependence of wind speed to building damage, asymmetries may need to be explicitly taken into account.

many years' worth of cyclone activity have to be evaluated in order to formulate a picture of the climatology, it is necessary to implement an automated and objective procedure using a dataset that spans many storms and many years yet at the same time provides sufficiently high resolution in order to accomplish the goal.

3. DATA AND METHODOLOGY

The JRA-25 Reanalysis dataset was used to identify asymmetries in the sea-level pressure distribution of typhoons in the Pacific. This dataset exists for the period 1979-2004. The pressure level (anl_p) version was used, which has a spatial resolution of 1.25 degrees and a temporal resolution of 6 hours. The JRA-25 Reanalysis data was supplemented with JMA Climate Data Assimilation System JCDAS data from 2005-2008 to provide a 30-year dataset. It was identical in spatial and temporal resolution to that of the JRA-25. Because the datasets were quite large to download, and because activity in the basin does not really begin until May, the months of January through March were not examined. This omitted fewer than 4% of all track points and less than 2% of all track points in latitude-longitude regions significant for Japan.

Best-Track Data from the JMA was used to identify the positions of typhoon (actually all named TCs) centers at six hourly times in the Northwest Pacific. For each track point, the JRA-25 data was regridded to 0.125 degrees resolution using the regrid function in GrADS (Graphical Analysis and Display System) over the region 100E-180E and 0N-65N. The regridding was done so that the central pressure values a set distance to the left and right of the track could be more easily and precisely located. Once the center of a typhoon was located within the regridded JRA-25 data, the direction of motion was determined using the location from the time in question to its location 6 h later. The direction of motion was then used to determine the left- and right-hand sides. The SLP was then obtained at a distance of 5 degrees outward from the center in the left- and right-directions as well as the north-south and east-west directions.

A total of 26,014 data points were examined. Typhoons with stronger winds on the left/right (Left Max/Right Max) were counted as those track points where the SLP on the left was at least 1 hPa higher/lower than it was on the right at a distance of 5 degrees latitude from the center. This strategy was compared with subjectively identifying such asymmetries using available surface analysis maps from the JMA and showed good agreement. Although the threshold of 1 mb/500 km seems arbitrary it is consistent with one's visual ability to subjectively identify the asymmetry on surface weather maps with isobars at 4 hPa contour intervals. A typical wind-Cp relationship can be used to convert this threshold or left-right difference (delta) in sea-level pressure into the impact on maximum wind speed assuming that such a relationship is still valid in this case and that the Cp difference between left and right at 500 km can instead be interpreted as a peripheral pressure difference. For example, a 1 hPa change in the peripheral pressure for a category 1 (Saffir Simpson) hurricane in the wind-Cp relationship derived by Atkinson and Holliday (1977), results in about a 2 kt difference in maximum gradient wind speed. Given the shape of many wind damage functions that are used in catastrophe models, this change in the wind speed can result in a 10-20% change in the damage (and hence the insured loss) for a given region near the radius of maximum winds.

In addition to the left-right track-perspective asymmetries, other asymmetries were logged using north-south and east-west SLP differences Δ_{slp} at 5 degrees. Figure 2 provides a schematic of the way in which the SLP values were recorded at each track point.

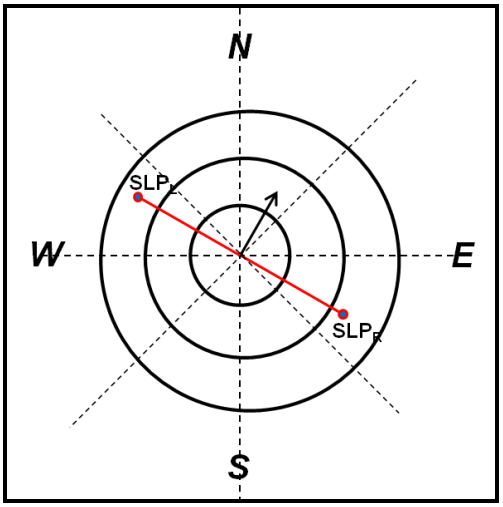

Fig. 2. Schematic showing how each storm track and sea-level pressure distribution was analyzed. The storm motion vector (black arrow) was based on subsequent 6-hour position and determined left- and right-directions. Sea-level pressures at a distance of 5 degrees exactly to the left and right (as indicated by red line segment) were recorded as well as values corresponding to S, SW, W, NW, N, NE, E, and SE directions.

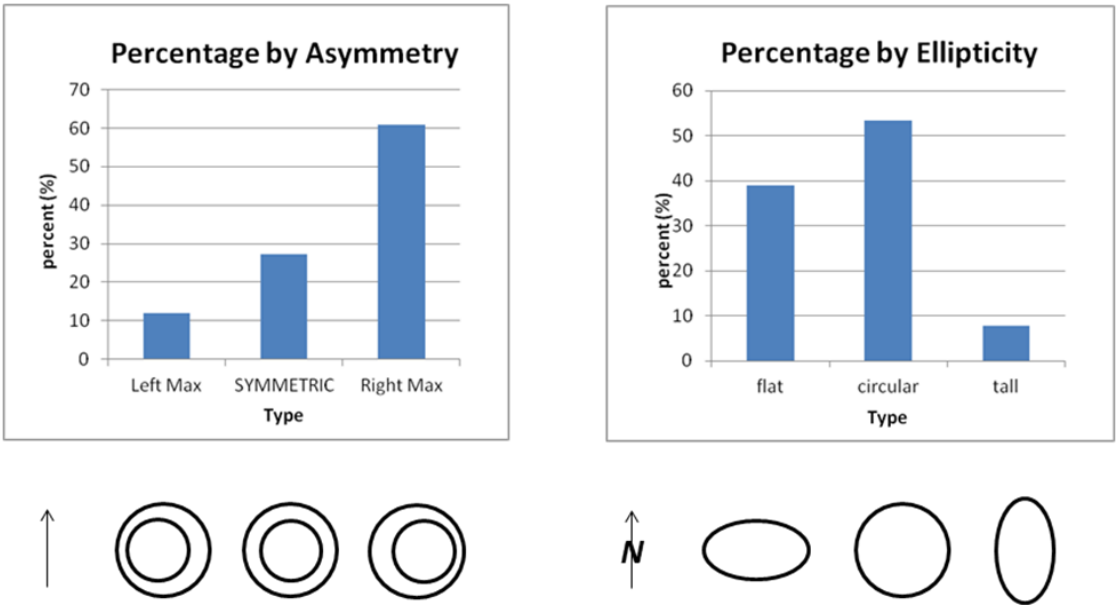

Fig. 3. Percentages of Left Max, SYMMETRIC, and Right Max track points found in the study (left panel). Percentages of flat, circular, and tall-elliptical track points found in the study (right panel). Asymmetric points determined relative to storm motion. Ellipticity points determined relative to geographic north. Circles and ovals below graphs represent isobars and indicate respective types.

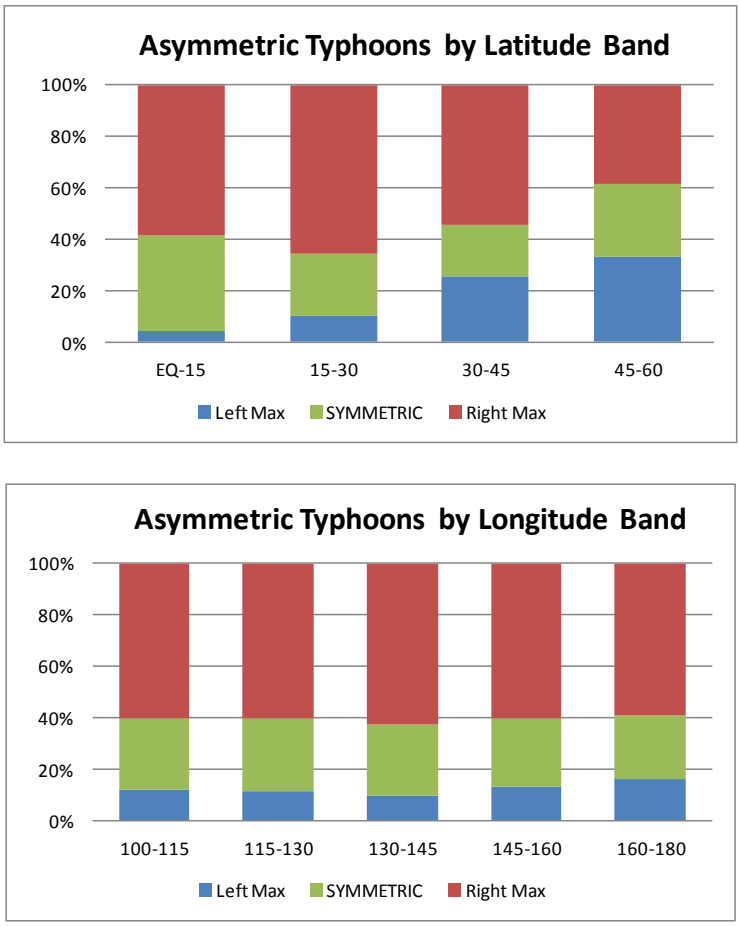

Fig. 4. Percentages of Left Max, SYMMETRIC, and Right Max track points by latitude band (upper panel) and longitude band (lower panel).

4. RESULTS

Of the 26,014 track points evaluated, 3,083 points were Left Max points and 13,106 points were Right Max ones. The remaining track points were classified as SYMMETRIC. Maximum wind speeds occurred on the left about 12% of the time, while maximum wind speeds occurred on the right about 61% of the time. Symmetric cases occurred about 27% of the time (see Fig. 3 - left panel). Although not the focus of this study, ellipticity measurements were logged so that analyses could be conducted later in more detail. For now, it can be said that almost 50% of the track points were classified either as flat ($\varepsilon < 0.8$) or tall ($\varepsilon > 1.25$) (see Fig. 3 – right panel). The ellipticity ε was determined based on the ratio of north-south Δ_{slp} to the east-west Δ_{slp} and can be interpreted as the ratio of the distance of the outermost closed isobar in the north-south direction to that in the east-west direction.

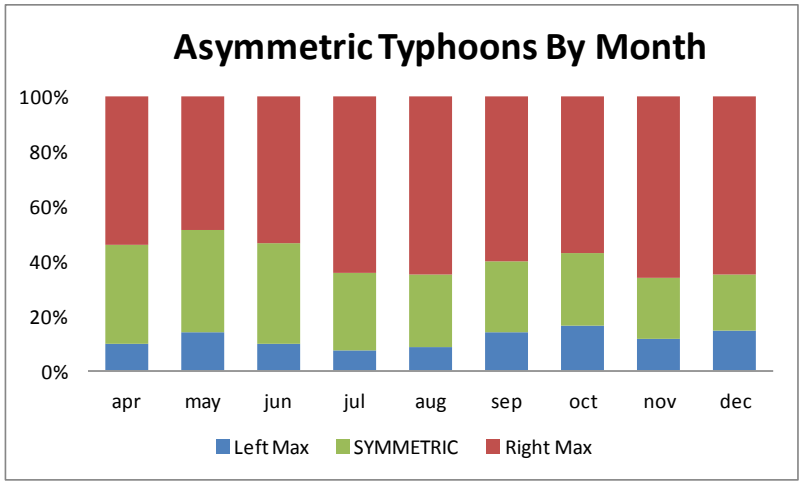

Fig. 5. Percentages of Left Max, SYMMETRIC, and Right Max track points by month. Study did not include activity during Jan-Mar.

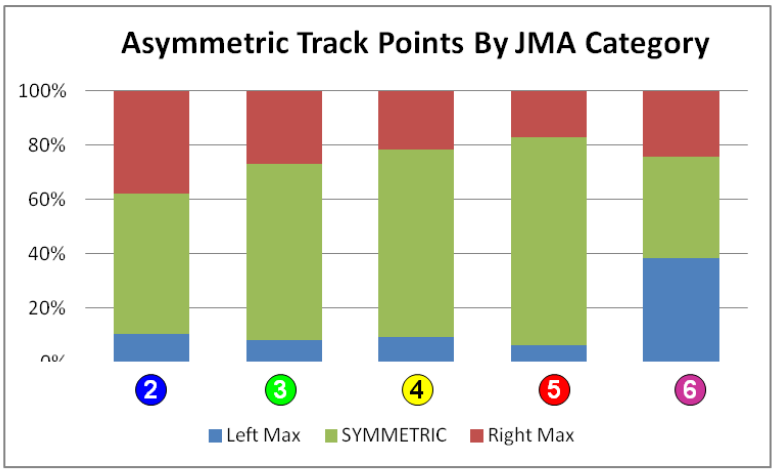

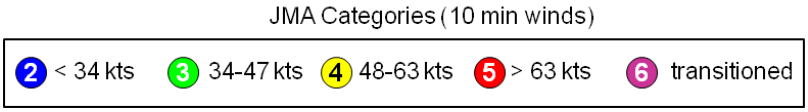

Fig. 6. Percentages of Left Max, SYMMETRIC, and Right Max track points by JMA intensity category as shown by colored circles. Wind speeds for categories are 10-min averages.

Figure 4 (upper panel) shows that most of the Left Max cases occurred more frequently north of 30 N – almost one-fourth of the time between 30-45 N and almost one-third of the time between 45-60 N. Figure 4 (lower panel) shows less dependence across longitude bands although there is a weak minimum in the percentage of Left Max points in the 130-145 E degree band. The distribution by month in Fig. 5 shows that the lowest frequency of Left Max cases occurred in July and increased steadily to a maximum frequency in October – with a large jump from August to September. The results in Figs. 4 and 5 support an explanation that is consistent with extratropical transitioning. Figure 6 shows the distribution of Left Max, Right Max, and SYMMETRIC percentages by JMA Intensity Category. The categories are defined in the Figure. The highest percentage indeed occurs in the XTT category. Otherwise, there is a slow decrease in frequency from the lowest intensity category (2) to the highest intensity one (5). Figure 7 shows the distribution of asymmetries according to the magnitude of asymmetry. Most of the Left Max points are in the 1-4 mb category

Max track point appeared in each cell was counted. The relative maximum (e.g., high percentage) in the grid cell defined by 30-45 N; 145-160 E is consistent with the results noted above. However, the absolute maximum for the domain is in a grid cell to the southwest. One of the reasons for this result is that this cell has the highest absolute track-point count. The Left Max percentage in the cell defined by 30-45 N; 130-145 E – at 25% - is particularly significant because it encompasses Japan. The significance is that for storms either making landfall along the southeastward facing coast of the main islands or brushing them to the south and east, a parametric wind calculation based on a circularly symmetric model may underestimate the winds on the left-hand side or overestimate them on the right-hand side one-fourth of the time. The same concern may be true for Taiwan and mainland China – albeit less frequently.

Figure 9 shows the storm intensity mode by grid cell. While it may not be so surprising that the most likely storm category for Left Max track points in the cell containing Japan is category 6

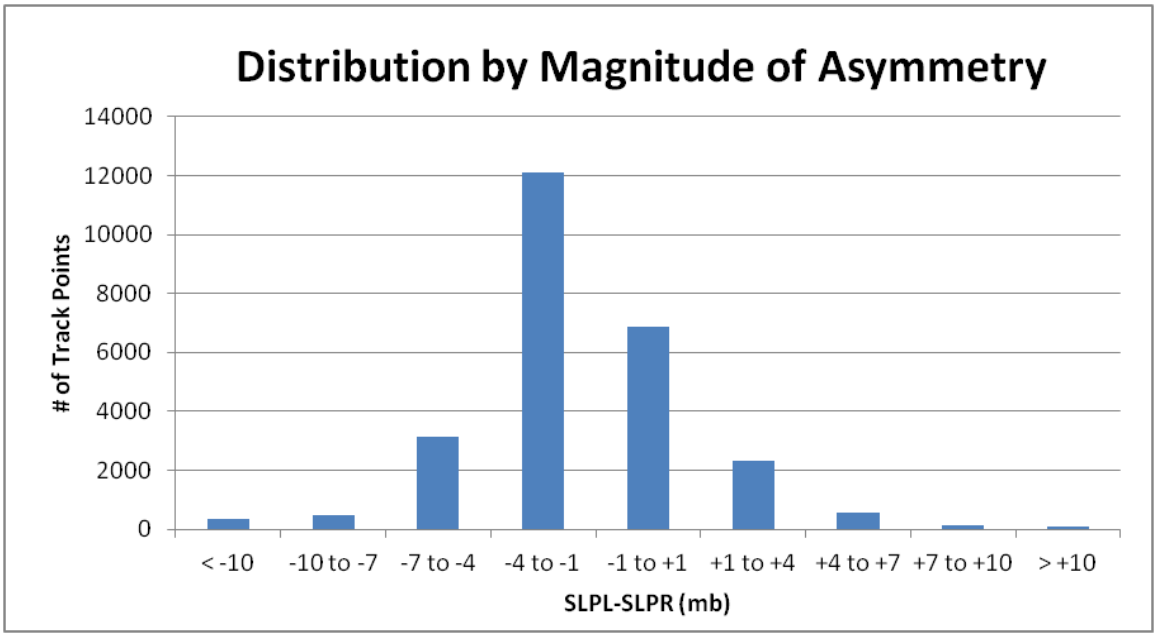

Fig. 7. Number of track points by left-right slp difference. Left Max points defined as those categories with positive differences beginning with +1 to +4 mb. Right Max points defined as those categories with negative differences beginning with -4 to -1 mb.

(75%). Higher magnitude Left Max asymmetries are much less common, with Left Max points of Δ_{slp} > 7 mb occurring 0.86% of the time.

Figure 8 shows the frequency of occurrence from a latitude-longitude perspective. Specifically, 15-degree latitude-longitude regions (cells) were considered and the number of times that a Left

(XTT), it is somewhat surprising that there is an almost equal likelihood of Category 2 through 5 for the cell containing Taiwan and China. Thus, there is a 0.25*0.12, or 3% chance that a JMA category 5 TC will affect Taiwan or China with strongest winds on the LHS, which is the side that will likely affect those landmasses first as it begins to recurve northeastward.

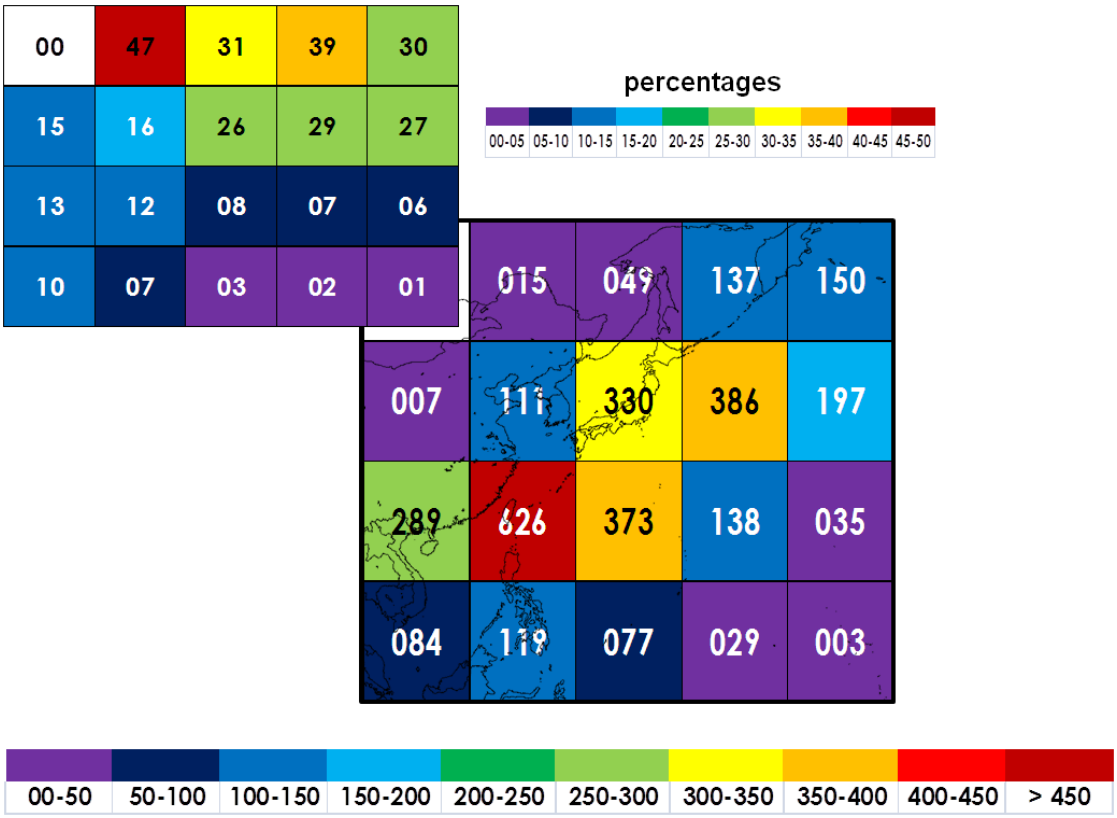

Fig. 8. Counts of Left Max track points by 15-degree latitude-longitude cell. Inset (upper left) shows corresponding percentages of occurrence.

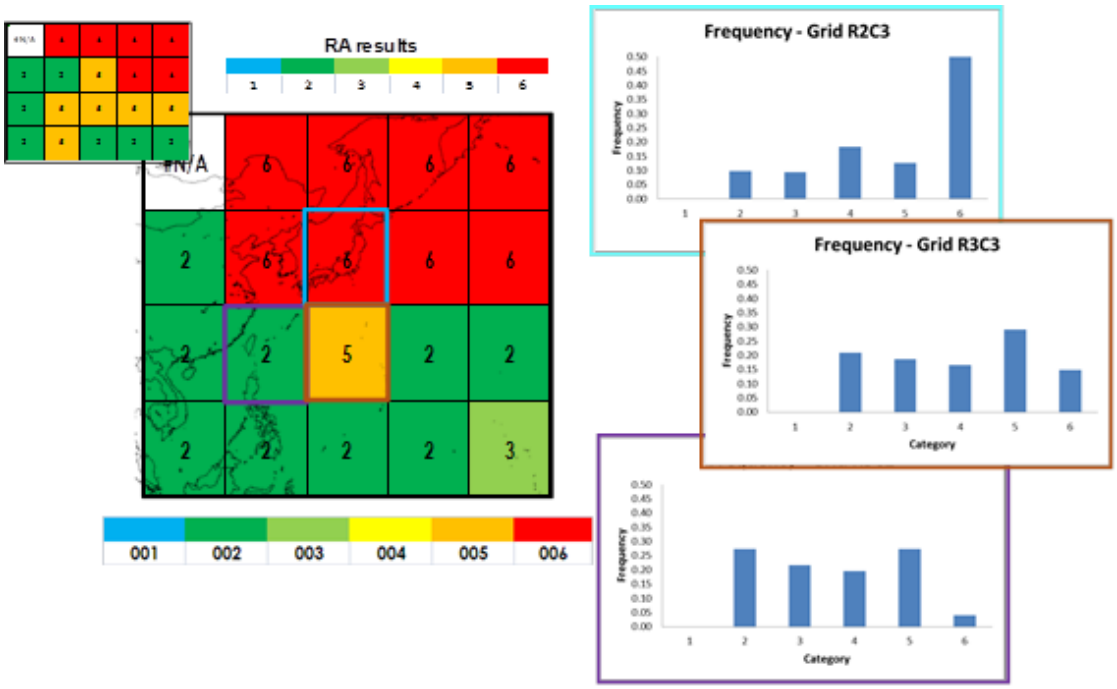

Fig. 9. Most likely storm category when track point is Left Max. Graphs to right show percentage breakdown for all storm categories for select grid cells as indicated by outline-color. Inset (upper left) indicates mode for Right Max track points.

Two regions with significant Left Max activity were evaluated in greater detail by creating composites of SLP, wind speed, and temperature for Left Max, Right Max, and SYMMETRIC events. Results for the region 30-35 N; 130-135 E are shown in Fig. 10. Not surprisingly, the Left Max composite shows a very mid-latitude cyclone like system. Strongest winds are visibly on the LHS, as determined by computing the gradient wind speed corresponding to the SLP distribution. Warm and cold fronts are even evident as enhanced regions of temperature gradient. The overlay of isobars and isotherms even suggests that frontogenesis is occurring as diffluent flow in the vicinity of strong temperature gradient further enhances the temperature gradient. These features are distinctly different from those for the SYMMETRIC and Right Max cases, as indicated in Table 1. Specifically, the Right Max composite moves more northerly at a slower speed in less baroclinicity. The SYMMETRIC case is right in between the Right Max and Left Max cases.

Figure 11 shows a similar composite – but for the grid cell 20-25 N; 120-125 E. This cell is centered approximately over Taiwan. The composite resembles that of the cell farther to the north and east but is less asymmetric and less elliptical. Interestingly it shows a forward velocity directed eastward, albeit very slow. The direction

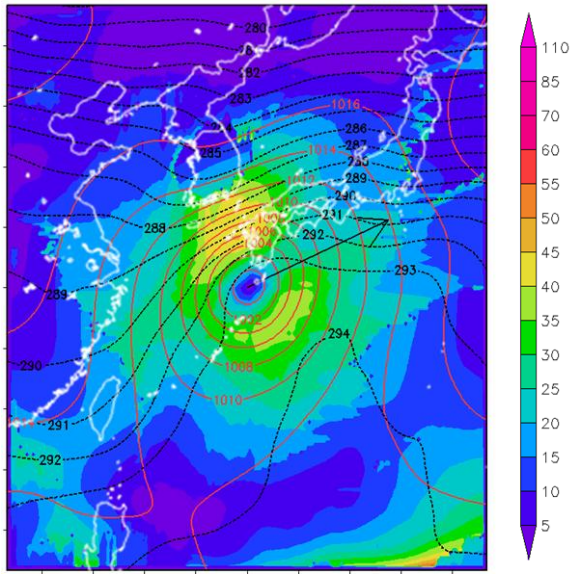

Fig. 10. Composite of Left Max track points for region 30-35 N; 130-135 E showing sea-level pressure (red contours); 850 hPa isotherms (black dashed contours); and gradient wind speed (color shading in knots) based on SLP contours. Arrow shows composite forward speed, which is 36 kph.

is consistent with the synoptic situation of a high pressure system to the northwest-over the Asian Continent moving southeastward–enhancing the SLP gradient on the left hand side of TCs and pushing them eastward. Table 2 summarizes the Right Max, SYMMETRIC, and Left Max statistics for this cell. Again, it can be seen that the SYMMETRIC composite is between the Right Max and Left Max ones. Interestingly the Right Max composite shows a northwestward velocity, which is consistent with the synoptic situation of a high pressure system centered east of the TC.

Table 1. Summary comparison of RIGHT Max, SYM, and LEFT Max composites for the Japan Case in the region 30-35N; 130-135E. Track points indicates number of points used in the composite, direction is storm motion clockwise from north, maxwnd is in kts, ΔT is a measure of the baroclinicity at 850 mb, and Cp and Pp are the central pressure and peripheral pressure (outermost closed isobar) respectively.

	RIGHT	SYM	LEFT
TrackPoints	168	43	38
FwdSpd (kph)	23	29	36
Direction	42	52	54
MaxWnd	40-45	40-45	45-50
ΔT (K)	6	9	14
C_p (hPa)	991	994	1000
P_p (hPa)	1002	1008	1010

5. SUMMARY AND DIRECTIONS OF FUTURE RESEARCH

Of the 26,014 track points evaluated, 3,083 points were Left Max points and 13,106 points were Right Max ones. Thus, maximum wind speeds occurred on the LHS about 12% of the time and maximum wind speeds occurred on the RHS about 61% of the time. Higher percentages for Left Max track points occurred farther north and along the eastern and western edges of the domain in late spring and early autumn. The high latitudes, the eastward locations that occur after recurvature, and the autumn time frame, are all features of storms that undergo XTT.

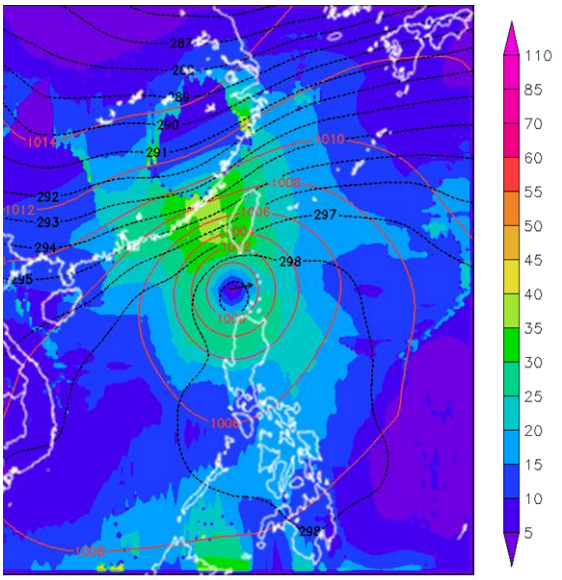

Fig. 11. Similar to Figure 12 but for the region 20-25 N; 120-125 E.

Table2. Similar to Table 1 but for Taiwan region.

	RIGHT	SYM	LEFT
TrackPoints	471	182	105
FwdSpd (kph)	13	3	5
Direction	300	30	80
MaxWnd	40-45	30-35	35-40
ΔT (K)	3	6	12
C_p (hPa)	993	997	999
P_p (hPa)	1004	1004	1008

Future research will focus on getting this information into catastrophe models. The coarseness of the results spatially, may be addressed by comparing the SLP patterns for Left Max and Right Max cases, with more detailed wind information. Such detailed wind information may be obtained from reconnaissance data for the North Atlantic. This strategy would require extending the results to that basin, which is easily accomplished given the global nature of the JRA-25 dataset. The results in this study may also be compared to other high-resolution wind analyses, such as those which are available from the Regional and Mesoscale Meteorology Branch (RAMMB). Once the high resolution signature that corresponds to these results can be identified, a stochastic model that accounts for the asymmetries that result from XTT or other interaction with approaching weather systems can be formulated.

Acknowledgements

We gratefully acknowledge the Computational and Information Systems Laboratory at the National Center for Atmospheric Research for providing the Japan Reanalysis Data.

REFERENCES

Atkinson, G. D., and C. R. Holliday, 1977: Tropical cyclone minimum sea level pressure /maximum sustained wind relationship for the Western North Pacific. *Mon. Wea. Rev.,* **105**, 421-427.

Chen, Y., and M. K. Yau, 2003: Asymmetric Structures in a Simulated Landfalling Hurricane. *J. Atmos. Sci.*, **60**, 2294-2312.

Frank, W. M., E. A. Ritchie, 1999: Effects of environmental flow upon tropical cyclone structure. *Mon. Wea. Rev.*, **127**, 2044–2061.

Klein, Peter M., Patrick A. Harr, Russell L. Elsberry, 2002: Extratropical transition of western north pacific tropical cyclones: midlatitude and tropical cyclone contributions to reintensification. *Mon. Wea. Rev.*, **130**, 2240–2259.

Onogi, K., and others, 2007: The JRA-25 Reanalysis. J. Meteo. Soc. Japan, 85, 369-432. Avail from: http://www.climateknowledge.org/reanalysis/Onogi_Japanese_Reanalysis_JMSJ_2007.pdf

Persing, J., M. T. Montgomery, R. E. Tuleya, 2002: Environmental interactions in the GFDL hurricane model for hurricane opal. *Mon. Wea. Rev.*, **130**, 298–317.

Schultz, Lori A., Daniel J. Cecil, 2009: Tropical cyclone tornadoes, 1950–2007. *Mon. Wea. Rev.*, **137**, 3471–3484.

Sousounis, P. J. and J. Butke 2010, "The Climatological Significance of Extratropical Transitioning on Typhoon Precipitation over Japan," *Proceedings of the 29th American Meteorological Society Conference on Hurricanes and Tropical Meteorology*, Tucson, Arizona, May 10-14, 2010. Available at http://ams.confex.com/ams/pdfpapers/169244.pdf.

Sousounis, P. J. and M. Desflots 2010, "Evaluating the Impacts of Extratropical Transitioning on Typhoon Losses via Synoptic Case Studies," *Proceedings of the 29th American Meteorological Society Conference on Hurricanes and Tropical Meteorology*, Tucson, Arizona, May 10-14, 2010. Available at http://ams.confex.com/ams/pdfpapers/169228.pdf.